

Corrosion Behaviour of Aluminium Alloy in Palm Oil Methyl Ester (B100)

W.B. Wan Nik^{a*}, S. Syahrullail^b, R. Rosliza^c, M.M. Rahman^d, M.F.R. Zulkifli^a

^aFaculty of Maritime Studies and Marine Science, Universiti Malaysia Terengganu, 21030 Kuala Terengganu, Malaysia

^bFaculty of Mechanical Engineering, Universiti Teknologi Malaysia, 81310 UTM Skudai, Johor, Malaysia

^cFaculty of Chemical Engineering Technology, TATI University College, Teluk Kalung, 24000 Kemaman, Terengganu, Malaysia

^dFaculty of Pharmacy, International Islamic University of Malaysia, 25200 Kuantan, Pahang, Malaysia

*Corresponding author: niksani@umt.edu.my

Article history

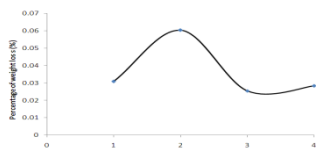
Received :15 June 2012

Received in revised form :12

August 2012

Accepted :28 August 2012

Graphical abstract



Abstract

The aim of this study is to determine the corrosion effect of palm oil methyl ester (POME) on aluminium alloy 5083 (AA5083). The static immersion test was carried out at 60°C for 68 days according to ASTM G-31-72. The corrosion analysis was done by using weight loss method and electrochemical test. The result from weight loss method shows the decreasing in weight loss of AA5083 which signifies the ability of POME to reduce corrosion rate. The electrochemical test shows the decreasing in polarization resistance, R_p , while the corrosion current densities, I_{corr} , increase. The corrosion rate reduces from 2.250mpy to 0.1946mpy. The low concentration of fatty acid C18:2 and high anti oxidant element contributes to the reduction of corrosion rate of AA5083 in POME.

Keywords: Aluminium alloy, corrosion, electrochemical impedance spectroscopy, palm oil methyl ester (POME), potentiodynamic polarization, weight loss

© 2012 Penerbit UTM Press. All rights reserved.

1.0 INTRODUCTION

Biodiesel are more likely getting the attention all over the world due to the energy needed and the environmental friendly properties. The use of the biodiesel could potentially reduce major pollutant substance in exhaust gases such as nitrogen oxide (NO_x), sulphur oxide (SO_x), carbon monoxide (CO), polycyclic aromatic hydrocarbons (PAHs), monocyclic aromatic hydrocarbons (MAHs), unburned hydrocarbon and other volatile gases [1]. The reduction in emissions was shown to be due to the desirable biodiesel properties such as higher oxygen content, lower sulphur and aromatic levels, and greater biodegradability when compared to fossil diesel [2,4].

Although biodiesel has a bright future as substitution of fossil fuel but the use of biodiesel still faces some challenges, including the problems of corrosion of fuel containers, low storage stability and oxidation stability of biodiesel [5]. Oxidative stability is the parameters that describe the degradation tendency of biodiesel and a great importance in content of possible problems with engine parts [6].

The vegetable-based which is palm oil methyl ester (POME) is mainly composed of fatty acids (e.g. palmitic acid, stearic acid, oleic acid, etc.), and some non-glyceride substances. The fatty acid composition of methyl esters of crude palm oil (CPO), crude palm stearin (CPS) and crude palm kernel oil (CPKO) is shown in Table 1.

Table 1 Comparison fatty acids composition (%) of the CPO, CPS, CPKO and CaroDiesel

	C12	C14	C16:0	C18	C18:1	C18:2	C20
CPO	0.3	0.8	44.3	5	39.1	10.1	-
CPS	0.4	1.9	52	4.1	32.7	7.9	-
CPKO	44.9	16	10.1	2.4	17.1	2.8	0.2
CaroDiesel	0.2	1	43.7	4.5	39.5	10.1	0.3

Biodiesel is non-toxic and can degrade about four times faster than fossil fuels and oxygen content improves the biodegradation process, leading to a decreased level of quick biodegradation [7]. This paper focused on the study of corrosiveness of POME towards AA5083 and four tests were conducted in order to complete this research.

2.0 MATERIALS AND METHODS

2.1 Sample Preparation

Aluminium Alloy (AA5083) specimens were cut into 25mm×25mm×3mm coupons for immersion tests. Before exposure, the samples were mechanically polished using 600 to

1500 silicon carbide (SiC) abrasive papers and lubricated using distilled water. The polished samples were cleaned with acetone, washed using distilled water, dried in air and stored over a desiccant [8].

2.2 Static Immersion Test

The static immersion tests were adapted from ASTM G-31-72 and carried out at 60°C for 1632 hours or around 68 days [9]. All test specimens were placed under the ambient condition. The aluminium alloy coupons were immersed into the beakers which contained biodiesel and it was placed in oil bath. The heating oil for oil bath is cooking oil. The cooking oil was used to compare the functional groups changes with the biodiesel. For the long-term static immersion test, biodiesel from each beaker was sampled and tested for acid value periodically throughout the test period.

2.3 Weight Loss Test

Specimens were weighed for the original weight and then hung in test solution for 68 days. The corroded specimens were then removed from the solutions, cleaned with distilled water and dried, then immersed in a nitric acid (HNO₃) for 2–3 min to remove the corrosion products. Finally, the coupons were washed with distilled water, dried and weighed again in order to obtain the final weight.

Corrosion rate is calculated assuming uniform corrosion over the entire surface of the coupon. Corrosion rates, CR are calculated from weight loss methods where W is the weight loss in milligrams, D is the metal density in g/cm³, A is the area of sample in cm², and T is the exposure period of sample in hours. Equation 1 was used to calculate corrosion rate [10]:

$$CR \left(\frac{\text{mm}}{\text{year}} \right) = 87.6 \times \left(\frac{W}{DAT} \right) \quad (1)$$

2.4 Impedance and Polarization Study

The potentiodynamic polarization study was conducted by using potentiostat. The cell used is a conventional three electrodes with a platinum wire counter electrode (CE) and a saturated calomel electrode (SCE) as reference to which all potentials are referred. The working electrode (WE) is in the form of a square cut so that the flat surface will be the only surface in the electrode. The potentiodynamic current-potential curves record the data after the electrode potential was automatically changed from -250mV to +250mV with the scanning rate of 5mVs⁻¹. The results were analyzed using the fit program GPES. Corrosion current (I_{corr}) was calculated by using the Stern-Geary equation as in Equation 2 where b_a is anodic Tafel slope, b_c is cathodic Tafel slope and R_p is polarization resistance [11,12]:

$$I_{corr} = \frac{b_c \times b_a}{2.303 R_p (b_c + b_a)} \quad (2)$$

Electrochemical impedance spectroscopy (EIS) study was done by using AC signal of impedance measurements by using potentiostat and run at the corrosion potential. All the potentials referred were relative to reference electrode which is saturated calomel electrode. The impedance measurements were conducted over a frequency range of 10⁻³ Hz to 10⁻¹ Hz. The results were analyzed using the fit program known as Frequency Response Analyzer (FRA).

3.0 RESULTS AND DISCUSSION

3.1 Weight Loss Test

The weight loss of AA5083 in POME has been determined as a function of the immersion time. Weight loss analysis can be seen in Figure 1. As seen, the highest weight loss was occurring at 2nd test and after that the weight loss start to decrease. At this point, the rate of metal dissolution was believed to be the highest. The oxidation process of POME might lead to the increasing of weight loss. Oxidation can lead to the formation of corrosive acids and deposits that may cause increased wear in engine parts [13]. The next test reveals that the weight loss of AA5083 keep reducing where at the 3rd test, it shows the lowest weight loss among others. The oxidation of POME at this point might be lower where it produces less corrosive acids and hence it reduces the weight loss of AA5083. Oxidation stability of vegetable oils depends on the level of unsaturated products presents. The lower the unsaturation the better oxidative stability but higher melting point [14]. This phenomenon signifies that POME has a tendency to retard the corrosion process and it is good for the development of biodiesel.

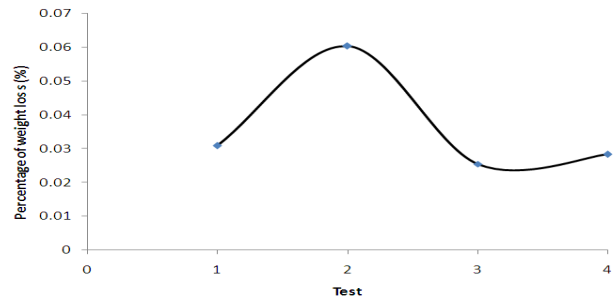


Figure 1 weight loss percentage of AA5083 immersed in POME

3.2 Electrochemical Impedance Spectroscopy

The impedance study can be seen in Figure 2a and the data is tabulated in Table 2. The graph was represented by single semicircle capacitive loop. As seen, the value of charge transfer resistance, R_{ct} for 1st test is the lowest and this value increases with respect to test period as can be obviously seen in Figure 2b. The smaller the semicircle is, the greater the corrosion rate will be [8]. Therefore, with the increasing test period apparently decrease the corrosion rate. The change of charge transfer resistance is due to charge transfer reaction and time constant of the electric double layer as well as surface inhomogeneity of structural or interfacial origin. The value of double layer capacitance, C_{dl} is illustrated in Figure 2c. From 1st to 3rd test, the value of double layer capacitance, C_{dl} decreases. The decrease in C_{dl} is due to the decrease in local dielectric constant and/or an increase in the thickness of the electrical double layer [15]. The 4th test shows there is an increment on C_{dl} value. The increasing of C_{dl} is due to the formation of porous layer of corrosion product on its surface and causes the increasing of local dielectric constant. When there are rises in dielectric constant value, the penetration of electrolyte through pores and cracks becomes greater. This considerable occurrence signifies that there are continuous diffusion of chloride ion at the metal/layer interface which subsequently causes the decreasing in R_{ct} and increasing in C_{dl} [16].

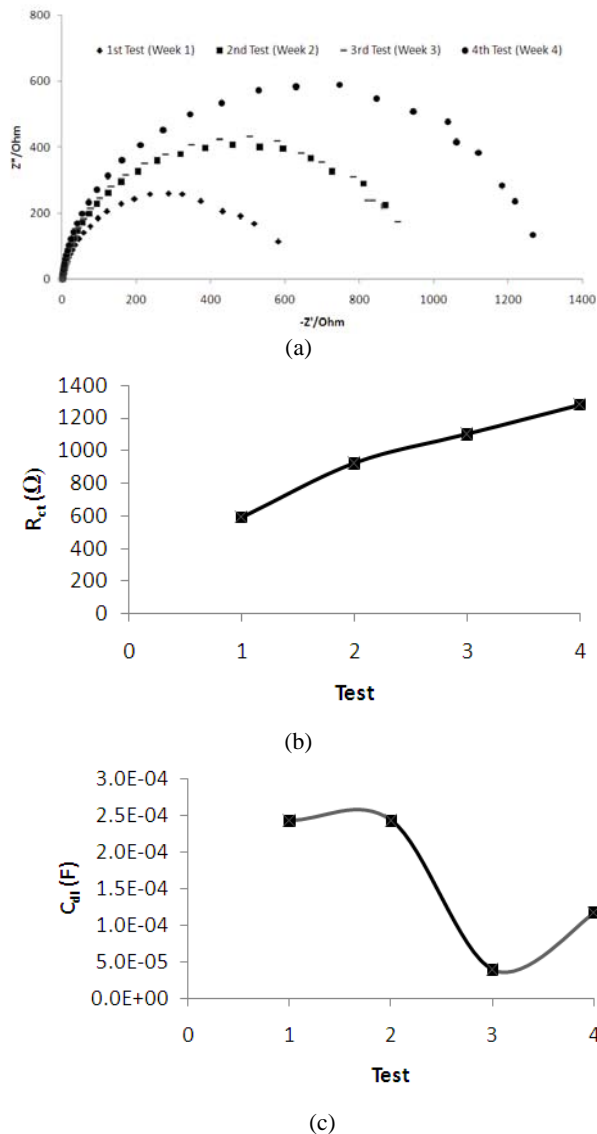


Figure 2 a) Nyquist plot for AA5083 immersed in POME b) Plot of charge transfer resistant, R_{ct} c) Plot of double layer capacitance, C_{dl}

Table 2 Impedance parameters gained from electrochemical impedance spectroscopy analysis

Test	$R_{ct}(\Omega)$	$C_{dl}(\text{F})$
1st Test	590.13	2.42E-04
2nd Test	920.04	2.42E-04
3rd Test	1097.98	3.92E-05
4th Test	1281.15	1.17E-04

3.3 Potentiodynamic Polarization Test

The value of I_{corr} is tabulated in Table 3. As seen in Figure 3 and Figure 4a, value of I_{corr} increases from 1st to 4th test. The increasing values of I_{corr} lead to the increasing of corrosion rate where at this point, the occurrence of cracks and pores can be detected. The existence of this cracks and pores allows the electrolyte to flow through it and directly react with metals where corrosion process begins to arise [17]. At this stage, the reaction is

controlled by activation energy of the reaction and consecutively the reaction later will be controlled by oxygen kinetics transport. As this reaction occur, the metals tend to lose its weight as this reaction is a function of surface roughness and dissolve oxygen and consequently increase I_{corr} at early immersion period. The value of E_{corr} gained from linear trend line decreasing with respect to test period as illustrated in Figure 4b. As the value of E_{corr} shifted to more negative value, the system tends to increase its metal dissolution and hydrogen evolution process [18].

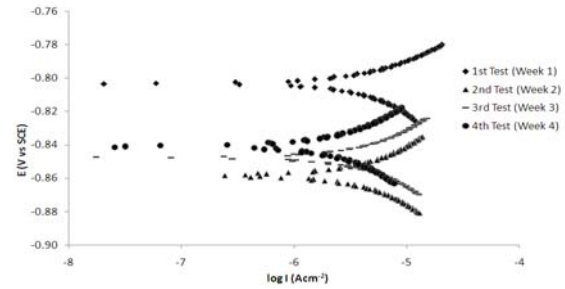


Figure 3 Tafel plots for AA5083

Table 3 Potentiodynamic polarization study parameters

Test	E_{corr} (mV)	b_c (mV/dec ⁻¹)	b_a (mV/dec ⁻¹)	I_{corr} (μAcm^{-2})
1st Test	-804	70	38	5.86
2nd Test	-858	93	59	6.41
3rd Test	-848	107	53	6.43
4th Test	-841	131	66	6.63

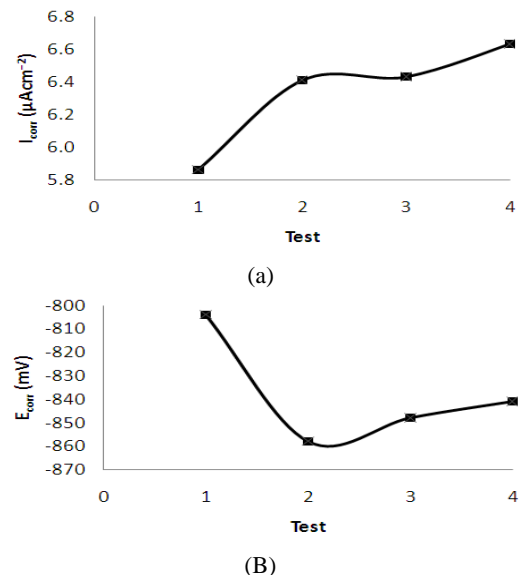


Figure 4 a) I_{corr} and b) E_{corr} plots of AA5083 in POME

4.0 CONCLUSION

Three types of test were conducted to study the corrosiveness of POME towards AA5083. Weight loss analysis shows reduction in weight loss while electrochemical and polarization test shows that the value of polarization resistance, R_p and charge transfer

resistance, R_{ct} increase while the value of double layer capacitance, C_{dl} decreases and the corrosion current density, I_{corr} also decreases and consequently reveals the ability of POME to retard the corrosion of AA5083.

Acknowledgement

The authors would like to express their deepest gratitude to Ministry of Higher Education for the fund provided (FRGS: Vot 59210) as well as the staff of Department of Maritime Technology and Department of Physical Sciences for their assistance.

References

- [1] J. H. Ng, H. K. Ng, S. Gan. 2009. Advances in Biodiesel Fuel for Application in Compression Ignition Engines. *Clean Tech Envi Policy*. DOI 10.1007/s 10098-009-0268-6.
- [2] M. A. Kalam, H. H. Masjuki. 2003. Exhaust Emission and Combustion Evaluation of Coconut Oil-Powered Indirect Injection Diesel Engine. *Journal of Renewable Energy*. 28(15): 2405–2415.
- [3] S. Kalligeros, F. Zannikos, S. Stourmas, E. Lois, G. Anastopoulos, C. Teas, F. Sakellariopoulos. 2003. An Investigation of Using Biodiesel/Marine Diesel Blends on the Performance of A Stationary Diesel Engine. *Biomass & Bioenergy*. 24(2): 141–149.
- [4] G. Labeckas, S. Slavinskas. 2006. Performance of Direct-Injection Off-Road Diesel Engine on Rapeseed Oil. *Journal of Renewable Energy*. 31(6):849–863.
- [5] Y. Boonyongmaneerat, C. Sukjamsri, U. Sahapatsombut, S. Saenapitak, S. Sukkasi. 2011. Investigation of Electrodeposited Ni-Based Coatings for Biodiesel Storage. *Journal of Applied Energy*. 88: 909–913.
- [6] G. Karavalakis, S. Stourmas, D. Karonis. 2010. Evaluation of the Oxidation Stability of Diesel/Biodiesel Blends. *Fuels*. 89: 2483–2489.
- [7] A. Demirbas. 2009. Progress and Recent Trends in Biodiesel Fuels. *Journal of Energy Conversion and Management*. 50: 14–34.
- [8] R. Rosliza, W.B. Wan Nik, H.B. Senin. 2008. The Effect of Inhibitor on the Corrosion of Aluminum Alloys in Acidic Solutions. *Materials Chemistry and Physics*. 107: 281–288.
- [9] A. S. M. A. Haseeb, S. Y. Sia, M. A. Fazal, H. H. Masjuki. 2010. Effect of Temperature on Tribological Properties of Palm Biodiesel. *Journal of Energy*. 35: 1460–1464.
- [10] P. Venkatesan, B. Anand, P. Matheswaran. 2009. Influence of Formazan Derivatives on Corrosion Inhibition of Mild Steel in Hydrochloric Acid Medium. *Journal of Chemistry*. 6(S1): 438–444.
- [11] H. Ashassi-Sorkhabi, D. Seifzadeh, M. G. Hosseini. 2008. En, Eis and Polarization Studies to Evaluate the Inhibition Effect of 3h-Phenothiazin-3-One, 7-Dimethylamin on Mild Steel Corrosion in 1 M Hcl Solution. *Corrosion Science*. 50: 3363–3370.
- [12] Z. T. Chang, B. Cherry, M. Marosszek. 2008. Polarization Behaviour of Steel Bar Samples in Concrete in Seawater Part 1: Experimental Measurement of Polarization Curves of Steel in Concrete. *Corrosion Science*. 50: 357–364.
- [13] R. Dinkov, G. Hristov, D. Stratiev, V.B. Aldayri. 2009. Effect of Commercially Available Antioxidants over Biodiesel/ Diesel Blends Stability. *Fuel*. 88: 732–737.
- [14] M. A. Maleque, H. H. Masjuki, S. M. Sapuan. 2003. Vegetable-based Biodegradable Lubricating Oil Additives. *Industrial Lubrication and Tribology*. 55(3): 137–143.
- [15] A. Singh, V. K. Singh, M. A. Quraishi. 2010. Aqueous Extract of Kalmegh (*Andrographis Paniculata*) Leaves as Green Inhibitor for Mild Steel in Hydrochloric Acid Solution. *International Journal of Corrosion*. 2010: 1–10.
- [16] G. Ruhi, O. P. Modi, A. S. K. Sinha, I. B. Singh. 2008. Effect of Sintering Temperatures on Corrosion and Wear Properties of Sol–Gel Alumina Coatings on Surface Pre-Treated Mild Steel. *Corrosion Science*. 50: 639–649.
- [17] N. F. Atta, A. M. Fekry, H. M. Hassan. 2011. Corrosion Inhibition, Hydrogen Evolution and Antibacterial Properties of Newly Synthesized Organic Inhibitor on 316L Stainless Steel Alloy in Acid Medium. *International Journal of Hydrogen Energy*. 36: 6462–6471.
- [18] A. Phanasaonkar, V. S. Raja. 2009. Influence of Curing Temperature, Silica Nanoparticles and Cerium on Surface Morphology and Corrosion Behaviour of Hybrid Silane Coatings on Mild Steel. *Surface & Coatings Technology*. 203: 2260–2271.